Published in final edited form as:
*Cell Rep*. 2012 January 26; 1(1): . doi:10.1016/j.celrep.2011.11.005.

# The NLRP3 Inflammasome Promotes Age-related Thymic Demise and Immunosenescence

**Yun-Hee Youm**[1], **Thirumala-Devi Kanneganti**[2], **Bolormaa Vandanmagsar**[1], **Xuewei Zhu**[3], **Anthony Ravussin**[1], **Ayinuer Adijiang**[1], **John S. Owen**[4], **Michael J. Thomas**[4], **Joseph Francis**[6], **John S. Parks**[3,4], and **Vishwa Deep Dixit**[1,6,5]

[1]Immunobiology Laboratory, Pennington Biomedical Research Center, Louisiana State University System, Baton Rouge, LA 70808

[2]Department of Immunology, St. Jude Children's Research Hospital, Memphis, TN, 38105

[3]Department of Pathology, Section on Lipid Sciences, Wake Forest School of Medicine, Winston-Salem, NC 27157

[4]Department of Biochemistry, Wake Forest School of Medicine, Winston-Salem, NC 27157

[6]Comparative Biomedical Sciences, School of Veterinary Medicine, Louisiana State University System, Baton Rouge, LA 70808

## Abstract

The collapse of thymic stromal cell microenvironment with age and resultant inability of the thymus to produce naïve T cells contributes to lower immune-surveillance in the elderly. Here we show that age-related increase in 'lipotoxic danger signals' such as free cholesterol (FC) and ceramides, leads to thymic caspase-1 activation via the Nlrp3 inflammasome. Elimination of Nlrp3 and Asc, a critical adaptor required for inflammasome assembly, reduces age-related thymic atrophy and results in an increase in cortical thymic epithelial cells, T cell progenitors and maintenance of T cell repertoire diversity. Using a mouse model of irradiation and hematopoietic stem cell transplantation (HSCT), we show that deletion of the Nlrp3 inflammasome accelerates T cell reconstitution and immune recovery in middle-aged animals. Collectively, these data demonstrate that lowering inflammasome-dependent caspase-1 activation increases thymic lymphopoiesis and suggest that Nlrp3 inflammasome inhibitors may aid the reestablishment of a diverse T cell repertoire in middle-aged or elderly patients undergoing HSCT.

### Keywords

Inflammation; T cells; CDR3; aging; adipocytes; macrophages; Pycard; IL-1β; caspase-1; ASC; Free Cholesterol; Ceramide; fatty acids; IL-7; epithelial cell; IL-18; apoptosis; stem cells; bone marrow; cancer; fatty acids



[5]Address and Correspondence to: Vishwa Deep Dixit, Ph.D, Laboratory of Neuroendocrine-Immunology, Pennington Biomedical Research Center, 6400 Perkins Road, Baton Rouge, LA 70808, Vishwa.Dixit@pbrc.edu, Phone: 225-763-2719, Fax: 225-763-0261.

## Introduction

Individuals aged 65 years or older constitute 12.9% of the US population, a number expected to increase to 71 million by 2030 (CDC, 2003). In addition, the number of persons aged ≥80 years is expected to increase from 9.3 million in 2000 to 19.5 million in 2030 (CDC, 2003). Intriguingly, thymic aging precedes that of several other organs and is a central feature and precursor of age-related deterioration in immune competence that appears in later life (Dorshkind et al., 2009; Chidgey et al., 2007).

In metabolically healthy individuals, by the age of 45 years, approximately 75% of the thymic microenvironment is composed of lipid-containing cells (Dixit, 2010). The early collapse of the thymic microenvironment or age-related thymic involution is characterized by loss of developing T cells, thymic epithelial cells (TECs) (Chidgey et al., 2007), increase in thymic fibroblasts (Yang et al., 2009), and emergence of lipid-laden cells (Dixit, 2010) via mechanisms that are still largely unclear. When the thymic lymphopoiesis or the thymic export of naïve T cells plummets, the total peripheral T cell pool is maintained through homeostatic expansion of pre-existing effector-memory T cells at the expense of naïve T cells in a thymus independent manner (Goronzy and Weyand, 2005). The consequent restriction of T cell diversity in aging is associated with increased risk and severity of emerging infections, certain cancers, and vaccination failures in the elderly (Maue et al., 2009). Furthermore, age-related thymic involution is a significant impediment to effective T cell reconstitution in middle-aged patients undergoing hematopoietic stem cell transplantations (HSCT) (Holland and van den Brink, 2009). Therefore, the ability to enhance thymic lymphopoiesis is thought to be central to the rejuvenation of T cell-mediated immune-surveillance in the elderly (Dorshkind et al., 2009; Chidgey et al., 2007; Holland and van den Brink, 2009; Holländer et al., 2010).

While reduction of stromal cell-derived intrathymic growth factors and alterations in extrinsic factors, such as circulating neuroendocrine hormones, play an important role in thymic involution, little is known about molecular triggers that cause thymic aging (Dorshkind et al., 2009; Dixit, 2010). Our prior studies have shown that partial reversal of age-related thymic involution by ghrelin, an agonist of growth hormone secretagogue receptor (GHSR), is associated with a reduction in the proinflammatory cytokine IL-1β (Dixit et al., 2004; Dixit et al., 2007). Consistent with the potential role of high levels of IL-1β in promoting thymic dysfunction, administration of IL-1β also induces marked thymic atrophy in mice (Morrissey et al., 1988a, Morissey et al., 1988b). However, it remains unclear whether the specific mechanisms that initiate the activation of IL-1β cause age-related thymic involution.

The cleavage of proIL-1β and proIL-18 into bioactive cytokines is predominantly dependent on caspase-1 (Kuida et al., 1995; Dinarello, 2009). The activation of caspase-1 zymogen into enzymatically active p20 and p10 heterodimers is, in turn, controlled by cytosolic multiprotein complexes called ‘inflammasomes’ (Martinon et al., 2002; Lamkanfi and Dixit, 2009). The Nlrp3 (nucleotide-binding domain, leucine-rich-containing family, pyrin domain-containing-3, also called Nalp3 and cryopyrin) inflammasome is formed via protein-protein interactions involving the pyrin domains of Nlrp3 and Asc (Mariathasan et al., 2004; Sutterwala et al., 2006; Martinon et al., 2009). The Asc protein serves as a key adaptor and binds with procaspase1 via CARD-CARD (caspase activation recruitment domain) interactions (Kanneganti et al., 2007; Latz, 2010). The Nlrp3 inflammasome can be activated by diverse ‘danger-associated molecular patterns’ (DAMPs) derived from damaged cells and organelles, and induces inflammation by secretion of IL-1β and IL-18 (Zhou et al., 2010; Duewell et al., 2010; Mariathasan et al., 2006). It is, however, unknown

whether such inflammasome-mediated sensing has a causal role in aging associated defects in thymic lymphopoiesis.

In our recent studies, we showed that deletion of Nlrp3 resulted in an unexpected increase in the number of naïve T cells in non-lymphoid organs such as subcutaneous adipose tissue (Vandanmagsar et al., 2011). These findings led us to hypothesize that the Nlrp3 inflammasome causes thymic involution by sensing an age-associated increase in intrathymic 'lipotoxic danger signals' and that dampening of Nlrp3 inflammasome activation may enhance naive T cell production by the thymus. Our current findings establish that Nlrp3 inflammasome-mediated sensing of age-related DAMPs, such as free cholesterol (FC) and ceramides within the thymic microenvironment, leads to caspase-1 activation. We show that lowering Nlrp3 inflammasome activity slows thymic aging and protects from subsequent T cell senescence.

## Results

### Nlrp3 Inflammasome senses aging-associated lipotoxic 'danger signals' in mouse thymus

Given that aging is associated with increases in several 'danger signals' associated with a chronic pro-inflammatory state, our initial studies examined whether caspase-1 processing is associated with thymic aging. We found a marked age-dependent, progressive increase in autocatalytic processing of inactive procaspase-1 into the active p20 caspase-1 heterodimer in thymus. This increase was apparent by 5–6 months of age and highest in 2 year old mice (Figure 1A and Supplementary Figure 1A). Our data revealed that Nlrp3 and IL-1β are highly expressed in thymic myeloid cells (TMCs:$CD45^{+}CD11c^{+}$) with low expression in thymocytes (CD45+$CD11c^{-}$) and thymic stromal cells (TSCs: $CD45^{-}CD11c^{-}$) (Figure 1B, C). Interestingly, the TSCs expressed the highest IL-1R (Figure 1C). The Asc/Pycard and IL-18 mRNA was expressed in all cell types examined (Figure 1B and Supplementary Figure 1B).

We next investigated the age-related DAMPs that cause caspase-1 activation. Interestingly, in contrast to young animals (1 month old), middle-aged mice (12 month old) had a significant increase in thymic concentration of potentially cytotoxic free cholesterol (FC) (Figure 1D). Immunostaining of thymic cryosections revealed that the majority of FC staining in the aging thymus was localized to $CD11b^{+}$ thymic macrophages in the medullary region (Figure 1E and Supplementary Figure 1D). Surprisingly, the thymic cholesterol ester content was reduced to undetectable levels with age (Supplementary Figure 1C). Interestingly, in the presence of elevated intracellular FC, LPS-primed bone marrow derived macrophages (BMDMs) displayed autocatalytic processing of caspase-1 (Figure 1F). The FC induced caspase-1 cleavage and IL-1β secretion in BMDMs was abolished in the absence of Nlrp3 (Figure 1G, H). Of note, this was not due to differences in FC loading or cholesterol ester content in the BMDMs of WT and *Nlrp3*$^{-/-}$ mice (Supplementary Figure 1E).

Aging is also associated with increase in 'danger signals' such as extracellular ATP from dead cells, by products of fatty acid metabolism such as ceramides, lipid peroxidation product like 4- hydroxynonenal (4HNE) and advanced glycation end products (AGE) (Wu et al., 2007; Ramasamy et al., 2005; Mattson 2009; Tucker & Turcotte 2003). We found that extracellular ATP and ceramides cause caspase-1 cleavage into enzymatically active p20 subunits, whereas AGE, 4HNE and fatty acids like palmitate, stearidonic acid (SDA), docosahexanoic acid (DHA) did not cause caspase-1 activation in macrophages (Figure 1I). Furthermore, the BMDMs deficient in Asc were not activated by C2 and C6 ceramide induced caspase-1 cleavage (Figure 1J) demonstrating that the Nlrp3 inflammasome specifically senses ceramides as lipotoxic 'danger signals'.

Measurement of ceramides in the thymus by liquid chromatography-mass spectrometry (LC/MS) revealed that compared to 2- month old animals, the total ceramide content was significantly increased in aged thymi (Figure 1K). Interestingly, similar to FC, we detected increased immunoreactivity for ceramides in the thymic medulla with pronounced co-localization in thymic macrophages ($CD11b^+$ and $F4/80^+$) Figure 1L, Supplementary Figure 2A, B). The intra-thymic delivery of C6 ceramide injection in young WT mice induces strong caspase-1 activation in thymus, which was substantially reduced in the absence of Nlrp3 (Figure 1M). These data suggest that increasing the ceramide content in thymus *in vivo* causes caspase-1 activation via the Nlrp3 inflammasome dependent mechanism.

## Nlrp3 inflammasome activation promotes age-related thymic involution

We next investigated whether the Nlrp3 inflammasome regulates the age-related increase in caspase-1 activation. Our data revealed that caspase-1 processing in thymi derived from 9-month old mice is dependent on Nlrp3 inflammasome activation (Figure 2A). Furthermore, the caspase-1 activation in 18-month old thymi was significantly attenuated in Nlrp3 deficient mice (Figure 2B and Supplementary Figure 3A). Consistent with these data, compared to 18-month old WT mice, IL-1β activation in thymi from Nlrp3 deficient mice was also considerably reduced (Figure 2C, Supplementary Figure 3B). IL-1 β levels in the plasma and sera of aged WT mice were below the detection limit of the assay (data not shown) suggesting that intra-thymic IL-1β and caspase-1 activation impacts the thymic involution process.

To determine a definitive causal relationship between inflammasome activation and age-related thymic involution, we investigated thymic mass (Figure 2D) and thymic cellularity (Figure 2E) in Nlrp3 and Asc deficient mice fed normal-chow diet and aged for 1, 5, 9, 18 and 23 months. Compared to young WT animals, neither Nlrp3 nor Asc deficient mice displayed any difference in thymic cellularity or thymic size (Figure 2D, E and Supplementary Figure 4). Concomitant with the timing and the degree of caspase-1 activation in thymus (Figure 1 A), the 5, 9, 18 and 23 month old *Nlrp3*$^{-/-}$ *and Asc*$^{-/-}$ showed significant protection from age-related decline in thymic mass and cellularity (Figure 2D, E). The evaluation of body composition by NMR imaging revealed no differences in normal chow-fed WT, Nlrp3 and Asc deficient mice at 1, 9, 18 and 23 months of age (data not shown), suggesting that changes in systemic adiposity do not account for the differences in the thymic involution.

The examination of thymic architecture revealed that, compared to age-matched WT controls, 14- and 23-month old *Nlrp3*$^{-/-}$ and *Asc*$^{-/-}$ mice displayed remarkable preservation of cortical and medullary cellularity (Figure 2F). In 14-month old WT mice, evidence of medullary fibrosis and presence of ectopic adipocytes in subcapsular cortical zones was clearly evident by H&E staining (Figure 2F). In contrast, thymic sections of 14-month old *Nlrp3*$^{-/-}$ and *Asc*$^{-/-}$ mice revealed clearly defined corticomedullary junctions and absence of adipogenic cells within thymic zones (Figure 2F). The Trichome staining revealed a considerable increase in subcapsular fibrosis and ectopic adipocytes in 14-month old WT mice; whereas, *Nlrp3*$^{-/-}$ mice had negligible subcapsular fibrosis, and the majority of extra-cellular matrix (ECM) was localized to the well-defined medullary regions (Figure 2G). By 23 months of age, the collapse of thymic architecture was more severe and was noticeable by loss of cortical areas, inversion of cortical-medullary zones, appearance of thymic cysts and an increase in thymic adipocytes (Figure 2H). Consistent with an increase in thymic cellularity, the histological examinations revealed that 23-month old *Nlrp3*−/− and *Asc*−/− mice were substantially protected from age-related thymic-involution (Figure 2H).

## Deletion of Nlrp3 inflammasome partially protects against age-related decline of TECs and T cell progenitors

The age-related reduction of thymic epithelial cells (TECs) and T cell progenitors are the major mechanisms that compromise naïve T cell export from thymus (Dorshkind et al., 2009; Chidgey et al., 2007; Holland and van den Brink, 2009). Consistent with increased inflammasome activation in aged thymus and high IL-1R in enriched TECs, we found that both *Nlrp3*$^{-/-}$ and *Asc*$^{-/-}$ mice exhibited a significant increase in cortical TECs (CD45$^{-}$MHCII$^{+}$Ly5.1$^{+}$) (Figure 3A) with no change in TEC frequencies at young ages (data not shown). The confocal analyses revealed that 18-month old *Asc*$^{-/-}$ mice have increased immunostaining for cTEC cells (Figure 3B). In addition, compared to WT controls, the TECs from the thymi of 12-month old *Nlrp3*$^{-/-}$ mice expressed significantly higher levels of IL-7 and stem cell factor (SCF) (Figure 3C). Consistent with these data, the thymi of *Nlrp3*$^{-/-}$ and *Asc*$^{-/-}$ mice have significantly higher expression of IL-7, IL-7R and SCF, suggesting a superior thymic stromal microenvironment favoring enhanced thymic lymphopoiesis (Figure 3D).

Compared to WT mice, ablation of Nlrp3 inflammasome components (Nlrp3 and Asc) at all ages examined did not affect the frequencies of CD4 single positive (SP), CD8SP or double positive (DP) cells suggesting no defects in T cell development or the number of T cell progenitors (data not shown). Interestingly, the thymi of aged (23m) *Nlrp3*$^{-/-}$ mice had a significant increase in the earliest thymocyte progenitors (ETP; Lin$^{-}$ CD117$^{+}$CD25$^{-}$) and double negative (DN2) cells (Lin$^{-}$CD117$^{+}$CD25$^{+}$) with no change in DN3 (Lin$^{-}$CD117$^{-}$CD25$^{+}$) and DN4 (Lin$^{-}$CD117$^{-}$CD25$^{-}$) T cell progenitors (Figure 4A, B).

Thymic lymphopoiesis is dependent on homing of hematopoietic stem cells (HSCs) from the bone marrow to the thymus (Bhandoola et al., 2007). We found that there was an age-dependent increase in inflammasome activation in bone marrow (Figure 4C). Compared to 23m-old WT mice, the *Nlrp3*$^{-/-}$ animals displayed significant increase in lymphoid primed multipotent progenitors (LPMP:Lin$^{-}$Sca1$^{+}$Kit$^{+}$Flt3$^{+}$) in bone marrow with no change in the more differentiated population of common lymphoid progenitors (CLPs; Lin$^{-}$Sca1$^{+}$Kit$^{lo}$CD127$^{-}$) (Figure 4D, E). In addition, ablation of Nlrp3 did not alter the frequency of other lineages tested including granulocyte-macrophage progenitor (GMP), common myeloid progenitor (CMP) and myelo-erythroid progenitors (MEP) populations in the BM (data not shown). Collectively, these data suggest that age-related Nlrp3 inflammasome activation may adversely impact thymic function by affecting the TECs and T cell progenitors in thymus and bone marrow.

## The inflammasome activation during aging induces immunosenescence

Consistent with no difference in thymic cellularity in 1m old mice, there was no change in naive CD4 and CD8 cell number between young WT mice and the Nlrp3−/− animals (Supplementary Figure 5A). Interestingly, as the effects of aging on erosion of naive T cell repertoire became evident in 9-month old WT mice, the age-matched *Nlrp3*$^{-/-}$ mice displayed a significant increase in CD4 and CD8 naïve T cells with lower effector-memory (E/M) populations (Figure 5A). Further analysis of 23-month old *Nlrp3*$^{-/-}$*and Asc*$^{-/-}$ mice revealed a pronounced increase in naïve T cells and a significant protection from age-related preponderance in E/M cells (Figure 5B).

Next, we quantified thymic T cell export by measurement of T cell receptor rearrangement excision circles (TREC), which are episomal byproducts of TCRδ locus excision during thymic TCRαβ re-arrangement (Douek et al., 1998). Under most conditions, TREC levels in the peripheral T cells directly correlate with production of new T cells by the thymus (Sempowski et al., 2002). Compared to WT mice, there was a significant increase in the

number of TRECs in CD4 cells of 9 and 18 month old Nlrp3 deficient mice (Figure 5D) suggesting increased thymic lymphopoiesis.

We next investigated whether the increased thymic export in *Nlrp3*$^{-/-}$ mice is associated with reduced T cell senescence, specifically lower antigen specific T cell proliferation and the restriction of TCR diversity. In contrast to T cells from aged WT mice, the T cells from 18-month (Supplementary Figure 5B) and 23- month old *Nlrp3*$^{-/-}$ mice exhibited significant increases in proliferation as well as IL-2 expression upon TCR ligation (Figure 5E, F). We studied the TCR diversity of peripheral CD4$^{+}$ T cells by measuring the distribution of lengths of the complementarity determining region 3 (CDR3) in 2 year old WT, *Nlrp3*$^{-/-}$ and *Asc*$^{-/-}$ mice (n =3/group). The TCR diversity is conferred due to VJ and VDJ gene recombinations in CDR3 region. Therefore, each Vβ-Jβ combination is represented as a Gaussian distribution of 6–10 CDR3 lengths with consecutive addition of 3 base pairs representing in-frame rearrangement (Pannetier et al., 1993; Nikolich-Zugich et al., 2004). As expected, in aged WT mice, TCR spectratyping revealed severe restriction in TCR repertoire that was represented by aberrant amplifications and deviation from a Gaussian distribution in all Vβ families (Figure 5G, Supplementary Figure 6). The CDR3 polymorphism analysis of age-matched old *Nlrp3*$^{-/-}$ and *Asc*$^{-/-}$ mice revealed substantial preservation of TCR repertoire diversity (Figure 5G, H and Supplementary Figure 6). Collectively, these data demonstrate that Nlrp3 inflammasome activation is a critical mechanism for the development of T cell senescence and T cell repertoire constriction during aging.

## Elimination of Nlrp3 inflammasome accelerates T cell reconstitution after HSCT

Age-related thymic involution is a significant impediment to effective T cell reconstitution in middle-aged and elderly patients that undergo hematopoietic stem cell transplantation (HSCT) as treatment for certain cancers (Holländer et al., 2010; Williams et al., 2007; Penack et al., 2010). We performed cytoablations using a radiation dose of 750cGy and syngeneic HSCT in 2- and 9 month old WT and Nlrp3 deficient mice to test whether the Nlrp3 inflammasome accelerates thymic recovery and immune reconstitution. Compared to WT mice, 2- month old *Nlrp3*$^{-/-}$ mice displayed no difference in thymic mass (Figure 6A) whereas, 9-month old *Nlrp3*$^{-/-}$ mice displayed significant increases in thymic size and cellularity (Figure 6A, 6B, 6C).

We next investigated whether the donor or host derived cells contribute towards changes in thymic reconstitution in 2- and 9 month old mice. There was no change in overall number of thymocyte subsets derived from host (CD45.2) or donor (CD45.1) origin HSC in 2-month old irradiated WT and *Nlrp3*$^{-/-}$ mice (Figure 6D and Supplementary Figure 7A). Interestingly, by 9 months of age, when age-related phase of thymic involution becomes more evident, the Nlrp3 deficient host microenvironment afforded a significant advantage to both the donor (CD45.1) and host (CD45.2) lineage of HSCs in their ability to reconstitute thymic cellularity (Figure 6D and Supplementary Figure 7A). Further analysis revealed that compared with 2-month old WT mice, there was a significant increase in thymocyte cell death (of both donor and host origin cells) in 9- month old animals (Figure 6E, Supplementary Figure 7B). In young animals, Nlrp3 deficiency had no impact on thymocyte death (Figure 6E). Interestingly, the age-related increase in thymocyte death in both host and donor lineage cells was substantially reduced in 9-month old Nlrp3 deficient mice (Figure 6E and Supplementary Figure 7B) suggesting that increased thymic cellularity in *Nlrp3*$^{-/-}$ mice after HSCT may be related to reduction in thymocyte death. Furthermore, 9 month old *Nlrp3*$^{-/-}$ mice had a significant increase in the frequency of naïve T cells in spleen 2 weeks after irradiation and HSCT (Figure 6F). In addition, compared to WT mice, the 9 month old *Nlrp3*$^{-/-}$ mice had significantly ($P<0.05$) higher total WBCs, lymphocyte counts, eosinophil

numbers and hematocrit (Figure 6G) with no difference in number of RBC, monocytes and hemoglobin (data not shown) in blood. Taken, together, these data demonstrate that Nlrp3 inflammasome is a critical regulator of radiation- induced injury to lymphoid organs and ablation of Nlrp3 increases T cell reconstitution in the clinical model of HSCT.

## Discussion

Current approaches for lifespan extension with the goal of compressing age-related morbidity draw on maintaining the function of all organs to optimal levels. However, in middle-aged healthy people, while the majority of other organs are functionally intact, the thymus is largely dysfunctional. Hence, thymic aging precedes development of later life immunosenescence, and age-related co-morbidities and approaches to delay thymic aging are thought to promote healthspan (Dorshkind et al., 2009). Results from human studies demonstrate that resection of thymus in children undergoing cardiac surgeries accelerates immunological aging and increases IL-1β (Sauce et al., 2009). Conversely, treatment of mice with IL-1β compromises thymic function (Morrissey et al., 1988a; Morrissey et al., 1988b). Here, we provide evidence that age-dependent Nlrp3 inflammasome activation impairs thymic lymphopoiesis by regulating intrathymic caspase-1 and IL-1β. We show that age-related increases in intrathymic ‘lipotoxic danger signals’ like free cholesterol and ceramides cause Nlrp3 inflammasome activation and participate in age-related thymic involution.

Nlrp3 expression is correlated with presence of CD11b positive cells in the thymus with the majority of expression in myeloid cells (Guarda et al., 2011). Importantly, Nlrp3 and IL-1β mRNAs were found to be mainly present in thymic myeloid cells; whereas, the IL-1β receptor was primarily expressed in enriched thymic epithelial cells (TEC) cell fractions. These findings suggest that age-dependent inflammasome-activation and production of IL-1β from thymic macrophages or dendritic cells may adversely impact the integrity of TEC compartment. Consistent with these data, elimination of the Nlrp3 inflammasome in aged mice prevented the age-related decline in cortical TECs, which was reflected in increased levels of the TEC-derived pro-thymopoietic cytokine IL-7.

Age-related activation of intrathymic caspase-1 and IL-1β is partly dependent on the Nlrp3 inflammasome. The aged Nlrp3- and Asc- deficient mice had a significant increase in naive T cells with reduction in effector-memory cells. In models of peritonitis and *in vitro*, the effector/memory (E/M) T cells appear to control inflammation by suppressing the activation of Nlrp3-inflammasome and secretion of IL-1β (Guarda et al., 2009). Our data shows that in control WT aged mice that display increases in E/M cells, there is also a progressive increase in Nlrp3 inflammasome dependent caspase-1 activation. These findings suggest that in aging, the expansion of E/M -T cells does not dampen Nlrp3 inflammasome activity. Also, the T cells of aged Nlrp3 inflammasome deficient mice displayed a broad TCR repertoire with increased expression of IL-2 and greater capability to proliferate in response to TCR ligation *in vitro*, suggesting lower T cell senescence.

The loss of thymic cellularity and perturbations in the thymic microenvironment are divided into development and aging-associated phases of involution (Shanley et al., 2009). The loss of thymic cellularity is apparent after birth, and the precise mechanisms responsible for the pre and post pubertal reduction in thymic cellularity and/or output versus age-related thymic involution are not fully understood. The 1-month old Nlrp3 and Asc deficient mice did not show any significant differences in thymic cellularity or T cell development stages suggesting that these mice do not have developmental defects and the development related decline in thymic cellularity is not dependent on inflammasome activation. The early phase of loss of thymic cellularity (which is not associated with any disease/stress) may be a

normal adaptive process as by 1.5 or 3 months of age in a mouse, a full repertoire of peripheral T cells is established and homeostatic mechanisms may suppress the production of additional T cells from thymus. Furthermore, since the early developmental phase is not associated with accumulation of lipotoxic danger signals, like FC and ceramides, the Nlrp3 inflammasome activation is relevant to regulating age-related inflammation and thymic involution.

The thymus, in particular, undergoes massive architectural changes with age (Dixit, 2010; Yang et al., 2009) that are associated with an age-related increase in lipid-containing cells. Aging is also associated with an increase in several potential DAMPs that can be sensed by inflammasomes. These activators include, but are not limited to, oxidative stress associated ROS, mitochondrial damage, by-products of fatty acid oxidation, lipid peroxidation, extracellular ATP derived from necrotic cells or alterations in autophagy. We found that the inflammasome was activated by increases in intracellular FC and ceramides but not by palmitate, 4HNE and AGE at the concentrations used. Recent studies showed that free cholesterol (FC) crystals that accumulate in macrophages activate the Nlrp3 inflammasome (Duewell et al., 2010). The majority of cholesterol in plasma is complexed with lipoproteins or stored in an inert-esterified state in cell cytosol. The levels of FC in cell membrane and endoplasmic reticulum are tightly regulated by pathways that control cholesterol efflux or esterification (Maxfield and Tabas, 2005). Increased levels of FC and ceramides in cells are thought to be cytotoxic (Maxfield and Tabas, 2005). Our data suggest that age-related accumulation of FC and ceramides in macrophages are sensed by the Nlrp3 inflammasome and may serve as an early pro-inflammatory trigger that impairs thymic lymphopoiesis.

The loss of thymic function with age significantly delays or compromises the establishment of diverse T cell repertoire in patients undergoing HSCT (Holländer et al., 2010; Williams et al., 2007). Rapid damage to thymocytes and thymic stroma by conditioning regimen of γ-radiation is well-documented (Holland and van den Brink, 2009; Williams et al., 2007). These data are also consistent with previous findings that IL-1β compromises the reconstitution of immune system after sublethal radiation and bone marrow transplantation (Morrissey et al., 1988a; Morrissey et al., 1988b). We found that elimination of Nlrp3 prevented thymocyte apoptosis and accelerated the thymic reconstitution in models of irradiation and HSCT. These findings suggest that in patients undergoing HSCT, the current cytoreductive clinical protocols could potentially be improved with anti-inflammatory therapy directed at blocking Nlrp3 inflammasome and IL-1β. Based on our data, it is likely that this new approach may significantly protect against thymic injury and could potentially accelerate the reconstitution of T cell repertoire through increased thymic lymphopoiesis in patients undergoing radiotherapy or HSCT.

Our study describes a fundamentally new mechanism whereby the Nlrp3 inflammasome controls the aging of thymus and leads to immune senescence. Current studies provide conclusive evidence that thymic aging can be substantially delayed by blocking the Nlrp3 inflammasome. However, an obvious caveat of aging studies in mouse models is the maintenance of animals in relatively calorie-dense, and sterile pathogen-free environment. Therefore, in current mouse models of aging, it is likely that ‘sterile or non-infectious’ inflammation drives several features of immunological aging and absence of the Nlrp3 inflammasome can therefore afford substantial protection to the thymus. Notably, the Nlrp3 inflammasome dependent innate immune response is required for efficient immune response to influenza and other infections (Pang and Iwasaki, 2011). Interestingly, early evidence suggests that Glyburide, an Nlrp3 inflammasome and $K^+$ ($K_{ATP}$) channel blocker (Lamkanfi et al., 2009), and a widely prescribed hypoglycaemic drug, affords substantial protection from gram-negative sepsis in diabetic patients (Koh et al., 2011). Therefore, the potential use of Nlrp3 inflammasome blockers or IL-1R antagonist such as Anakinra in age-related

degenerative disorders and thymic reconstitution deserves careful investigation. Our findings suggest that pharmacological Nlrp3 inflammasome blockers that specifically target the thymus may delay immunosenescence, maintain a diverse T cell repertoire and enhance immune-reconstitution in elderly patients.

## Material and Methods

### Mice and animal care

The *Asc*$^{-/-}$*and Nlrp3*$^{-/-}$ mice have been described previously (Mariathasan et al., 2004; Mariathasan et al., 2006). The mice were fed *ad libitum* with a normal chow diet consisting of 4.5% fat (5002; LabDiet) and aged in specific-pathogen free animal facility in ventilated cage racks that delivers HEPA filtered air to each cage. All transgenic and WT mice in our colony were cross-fostered to our parent cohorts. The sentinel mice in our animal rooms were negative for currently tested standard murine pathogens (Ectromelia, EDIM, LCMV, *Mycoplasma pulmonis*, MHV, MNV, MPV, MVM, PVM, REO3, TMEV and Sendai virus) at various times while the aging studies were performed (RADIL, Research Animal Diagnostic Laboratory, Columbia, MO).

The lethal irradiation to ablate hematopoietic cells was performed using X-Rad300, Xray small animal irradiator. One week before irradiation, the recipient mice were be given acidified, antibiotic water. The lineage depleted bone marrow cells from CD45.1$^{+}$ (B6.SJL$^{\text{Ptprca Pep3b/BoyJ}}$) were transplanted to irradiated (750cGy) syngeneic WT and *Nlrp3*$^{-/-}$ mice via tail vein injection. The mice were sacrificed 2 week after the HSCT for analysis of T cell reconstitution. Blood was collected through cardiac puncture in EDTA coated vials and analyzed for complete blood counts using automated CBC analyzer (Beckman Coulter DxH). All experiments were in compliance with the NIH Guide for the Care and Use of Laboratory Animals, which were approved by the Institutional Animal Care and Use Committee at Pennington Biomedical Research Center.

### Intrathymic injection

Mice were pre-medicated with atropine sulfate (0.04 mg/kg) and anesthetized 5 min later with 2% v/v isoflurane/oxygen. Mice were placed on a heating pad in supine position and the trachea was intubated using a 24-guage intravenous catheter with a blunt end. Anesthesia was maintained by supplementing oxygen (1.8 L/min) and 0.7%−2.0% isoflurane at a rate of 105/min and with a tidal volume of 2.1–2.5 ml using a rodent ventilator (Harvard Apparatus, Inc., MA). A left lateral thoracotomy was performed by blunt incision at the level of third intercostals space, the left thymus was visualized with the aid of a dissecting microscope (Zeiss) and exteriorized using a forceps. Then 50μl of ceramide or its vehicle alcohol was injected using a Hamilton syringe. The right thymus was used as control. The left thymus was returned to the thoracic cavity, the chest wall was closed, and the mouse was allowed to recover. The animals were sacrificed at 1h after intrathymic injections, both the left and right thymus were separated and snap frozen in liquid nitrogen and stored in −80ºC until analyzed for caspase-1 activation using Western blotting. All experiments were in compliance with the NIH Guide for the Care and Use of Laboratory Animals, which were approved by the Institutional Animal Care and Use Committee of LSU School of Veterinary Medicine and Pennington Biomedical Research Center.

### Flow cytometry

The ETPs and naive/memory T cell subpopulations were analyzed as previously described (Yang et al., 2009; Min et al., 2004). For Lin$^{-}$Sca1$^{+}$ckit$^{+}$ (LSK) cells analysis, thymocytes are stained for lineage negative cells followed by staining with FITC-conjugated anti-Sca1 and FITC-conjugated anti-c-kit (ebioscience) followed by staining for Flt3 (APC). The

thymocytes were stained for Annexin-V according to manufacturer's instructions (eBioscience). All the FACS data was analyzed by post collection compensation using FlowJO (Treestar Inc) software.

### Free Cholesterol and Ceramide measurement

To measure cholesterol content in macrophages and the thymus, the cellular lipids were extracted with isopropanol (including 5α-cholestane as internal standard) at room temperature overnight and analyzed for cholesterol content by gas-liquid chromatography (GLC) as described previously (Furbee et al., 2002). The thymic ceramide analyses were based on studies described previously (Hammad et al., 2010). The lipids from flash frozen thymi were extracted using the method of Folch et al., 1957, in the presence of 500 pmol of 12:0 ceramide as an internal standard. The ceramide fraction was separated using 500 mg amino-SPE columns (Bodennec et al., 2000). After concentration the samples were taken up in 1 ml of chloroform:methanol (3:1 ; v/v) containing 1mM lithium hydroxide. Ceramides were analyzed by direct infusion at 5 μL/min into a TSQ Discovery Max LC/MS/MS running in the positive ion mode. Individual ceramide species were detected in the mixtures by the common neutral loss of 48 Da from the lithiated ceramides.

### Macrophage culture and cytokine analysis

The murine bone marrow derived macrophages (BMDM) and cultured them according to previously established protocols (Mariathasan et al., 2006; Vandanmagsar et al., 2011). Cholesterol loading and LPS stimulation of macrophages- BMDMs were incubated with or without MβCD -cholesterol (final cholesterol concentration: 80mg/ml; Sigma) at 37°C for 1 h or with LPS for 6h. Then, culture supernatant was used for quantification of IL-1β by ELISA and cells were lysed in RIPA buffer containing complete protease inhibitor cocktail (Sigma) and used for Western Blot analysis.

### Western Blot Analysis

We conducted the immunoblot analysis for caspase-1, IL-1β in BMDMs, thymus, spleen and bone marrow as described previously[29]. The protein immune complexes were detected using specific fluorescent secondary antibodies conjugated with IRDye™800CW (Rockland) and membranes were imaged using Odyssey Infrared Imaging System (LI–COR Odyssey BLOT) or through ECL based detection method.

### T cell proliferation

The T cells were prepared using mouse negative selection columns (R&D Systems) and cultured on anti-CD3 and anti-CD28 coated plates (BD Pharmingen). The proliferation was analyzed using MTT assay according to manufacturer's instructions. The total RNA from unstimulated and stimulated T cells was used for IL-2 real time PCR analysis.

### Quantitative Real-time PCR

The total RNA from thymus and sorted thymocytes, TMs, and enriched TECs was prepared using RNeasy Mini Kit (Qiagen). All samples were DNAse digested to remove potential genomic DNA contamination. We conducted the Quantitative Real-time PCR as described previously (Vandanmagsar et al., 2011).

### Histology and Immunohistochemistry

The thymi obtained from mice were either fixed in 4% formalin and paraffin embedded (FFPE) or flash frozen and subsequently embedded in Stephens Scientific Frozen Section Medium (Riverdale, NJ) and cut into 5-μm-thick cryostat sections. At least three crysection serial sections were utilized for each staining. The FFPE sections were stained with

hematoxylin and eosin using autostainer (Dako) and fibrosis was analyzed by Trichome staining. The frozen sections were stained with anti-ceramides antibody and free cholesterol was detected using filipin labelling. The cortical and medullary TEC were stained with unconjugated rat mAb to TROMA-1 (DSHB, Hybridoma Bank, University of Iowa); biotin-conjugated mouse mAb to UEA-1 (Vector Labs) as described previously (Yang et al., 2009). Images were acquired using a Zeiss 510 Meta multiphoton confocal microscope.

### Quantification of signal joint T cell receptor excision circles

$CD4^+$ T subsets were isolated from splenocytes using mouse CD4+ T cells positive section kit (Invitrogen). The PCR was performed with mδRec and ψJα specific primers and mδRec-ψJα fluorescent probe as described previously (Yang et al., 2009). The standard curves for murine TRECs were generated by using δRec ψJα TREC PCR product cloned into a pCR-XL-TOPO plasmid.

### Vβ TCR spectratyping analysis

For TCR spectratyping and CDR3 length analysis PCR, a FAM-labeled nested constant β-region primer is used in combination with 24 multiplexed forward murine Vβ-specific primers. PCR was performed for 35 cycles with denaturation at 94°C for 30sec, annealing for 55°C for 30 sec and 1 min extension at 72°C and the PCR products are analyzed on ABI3130 genetic analyzer as described previously (Yang et al., 2009; Dixit et al., 2007).

### Statistical Analyses

We used a two–tailed Student's t test to determine significance in differences between genotypes or treatments; $*P < 0.05$ and $P < 0.01$, $**P < 0.005$ and $P < 0.001$. We expressed the results as the mean ± SEM or the mean ± SE. The differences between means and the effects of treatments were also analyzed by one–way ANOVA using Tukey's test (Sigma Stat), which protects the significance ($P < 0.05$) of all pair combinations.

## Supplementary Material

Refer to Web version on PubMed Central for supplementary material.

## Acknowledgments

We thank Vishva M. Dixit at Genentech Inc. for providing the anti-Caspase-1 antibody, $Asc^{-/-}$ and $Nlrp3^{-/-}$ mice, and Gregory D. Sempowski at Duke University School of Medicine for providing the TREC δRec ψJα plasmid. We thank Donald K. Ingram for helpful discussions, Michael Salbaum and David Burk in PBRC for technical assistance with thymic imaging. The research in Dixit Laboratory is supported in part by the National Institute on Health (R01AG31797, R01DK090556), Coypu Foundation and Pennington Biomedical Research Foundation. T.D.K. was supported by NIH grant AR056296. J.S.P was supported in part by HL49373, HL94525 and X.Z was supported by AHA (09POST2250225). The present work utilized the facilities of the Genomics and Cell Biology & Bioimaging Core facilities supported by NIH Grant 1 P20 RR02/1945. The Discovery Max tandem mass spectrometer was purchased with funds from North Carolina Biotechnology Center grant 2007-IDG-1021 (MJT). The MS analyses were performed in the Mass Spectrometer Facility of the Comprehensive Cancer Center of Wake Forest University School of Medicine supported in part by NCI center grant 5P30CA12197. None of the authors of this manuscript have a financial interest related to this work.

## References

Bhandoola A, von Boehmer H, Petrie HT, Zúñiga-Pflücker JC. Commitment and developmental potential of extrathymic and intrathymic T cell precursors: plenty to choose from. Immunity. 2007; 26:678–689. [PubMed: 17582341]

Bodennec J, Brichon G, Zwingelstein G, Portoukalian J. Purification of sphingolipid classes by solid phase extraction wioth aminopropyl and weak cation exchange cartridges. Methods Enzymol. 2000; 312:101–114. [PubMed: 11070865]

CDC. Public Health and Aging: Trends in Aging --- United States Worldwide. MMWR. 2003; 52:101–106. [PubMed: 12645839]

Chidgey A, Dudakov J, Seach N, Boyd R. Impact of niche aging on thymic regeneration and immune reconstitution. Semin Immunol. 2007; 19:331–340. [PubMed: 18024073]

Dixit VD. Thymic fatness and approaches to enhance thymopoietic fitness in aging. Curr Opin Immunol. 2010; 22:521–528. [PubMed: 20650623]

Dixit VD, Schaffer EM, Pyle RS, Collins GD, Sakthivel SK, Palaniappan R, Lillard JW Jr, Taub DD. Ghrelin inhibits leptin- and activation-induced proinflammatory cytokine expression by human monocytes and T cells. J Clin Invest. 2004; 114:57–66. [PubMed: 15232612]

Dixit VD, Yang H, Sun Y, Weeraratna AT, Youm YH, Smith RG, Taub DD. Ghrelin promotes thymopoiesis during aging. J Clin Invest. 2007; 117:2778–2790. [PubMed: 17823656]

Dorshkind K, Montecino-Rodriguez E, Signer RA. The ageing immune system: is it ever too old to become young again? Nat Rev Immunol. 2009; 9:57–62. [PubMed: 19104499]

Douek DC, McFarland RD, Keiser PH, Gage EA, Massey JM, Haynes BF, Polis MA, Haase AT, Feinberg MB, Sullivan JL, et al. Changes in thymic function wioth age and during the treatment of HIV infection. Nature. 1998; 396:690–695. [PubMed: 9872319]

Duewell P, Kono H, Ravner KJ, Sirois CM, Vladimer G, Bauemfeind FG, Abela GS, Franch L, Núñez G, Schnurr M, et al. NLRP3 inflammasomes are required for atherogenesis and activated by cholesterol crystals. Nature. 2010; 464:1357–1361. [PubMed: 20428172]

Folch J, Lees M, Sloane GH, Stanley A. A simple method for the isolation and purification of total lipides from animal tissues. J Biol Chem. 1957; 226:497–509. [PubMed: 13428781]

Furbee JW Jr, Sawyer JK, Parks JS. Lecithin:cholesterol acyltransferase deficiency increases atherosclerosis in the low density lipoprotein receptor and apolipoprotein E knockout mice. J Biol Chem. 2002; 277:3511–3519. [PubMed: 11719520]

Goronzy JJ, Weyand CM. T cell development and receptor diversity during aging. Curr Opin Immunol. 2005; 17:468–475. [PubMed: 16098723]

Guarda G, Dostert C, Staehli F, Cabalzar K, Castillo R, Tardivel A, Schneider P, Tschopp J. T cells dampen innate immune responses through inhibition of NLRP1 and NLRP3 inflammasomes. Nature. 2009; 460:269–273. [PubMed: 19494813]

Guarda G, Zenger M, Yazdi AS, Schroder K, Ferrero I, Menu P, Tardivel A, Mattmann C, Tschopp J. Differential Expression of NLRP3 among Hematopoietic Cells. J Immunol. 2011; 186:2529–2534. [PubMed: 21257968]

Hammad SM, Pierce JS, Soodavar F, Smith KJ, Al Gadban MM, Rembiesa B, Klein RL, Hannun YA, Bielawski J, Bielawska A. Blood phingolipidomics in healthy humans: Impact of sample collection methodology. J Lipid Res. 2010; 51:3074–3087. [PubMed: 20660127]

Holland AM, van den Brink MR. Rejuvenation of the aging Tcell compartment. Curr. Opin Immunol. 2009; 21:454–459.

Holländer GA, Krenger W, Blazar BR. Emerging strategies to boost thymic function. Curr Opin Pharmacol. 2010; 10:443–453. [PubMed: 20447867]

Kanneganti TD, Lamkanfi M, Núñez G. Intracellular NOD-like receptors in host defense and disease. Immunity. 2007; 27(4):549–559. [PubMed: 17967410]

Koh GC, Maude RR, Schreiber MF, Limmathurotsakul D, Wiersinga WJ, Wuthiekanun V, Lee SJ, Mahavanakul W, Chaowagul W, Chierakul W, et al. Glyburide Is Anti-inflammatory and Associated with Reduced Mortality in Melioidosis. Clin Infect Dis. 2011 (Epub ahead of print).

Kuida K, Lippke JA, Ku G, Harding MW, Livingston DJ, Su MS, Flavell RA. Altered cytokine export and apoptosis in mice deficient in interleukin-1 beta converting enzyme. Science. 1995; 267:2000–2003. [PubMed: 7535475]

Lamkanfi M, Dixit VM. Inflammasomes: guardians of cytosolic sanctity. Immunol Rev. 2009; 227:95–105. [PubMed: 19120479]

Lamkanfi M, Mueller JL, Vitari AC, Misaghi S, Fedorova A, Deshayes K, Lee WP, Hoffman HM, Dixit VM. Glyburide inhibits the Cryopyrin/Nalp3 inflammasome. J Cell Biol. 2009; 187:61–70. [PubMed: 19805629]

Latz E. The inflammasomes: mechanisms of activation and function. Curr. Opin Immunol. 2010; 22:28–33.

Mariathasan S, Newton K, Monack DM, Vucic D, French DM, Lee WP, Roose-Girma M, Erickson S, Dixit VM. Differential activation of the inflammasome by caspase-1 adaptors ASC and Ipaf. Nature. 2004; 430:213–218. [PubMed: 15190255]

Mariathasan S, Weiss DS, Newton K, McBride J, O'Rourke K, Roose-Girma M, Lee WP, Weinrauch Y, Monack DM, Dixit VM. Cryopyrin activates the inflammasome in response to toxins and ATP. Nature. 2006; 440:228–332. [PubMed: 16407890]

Martinon F, Burns K, Tschopp J. The inflammasome: a molecular platform triggering activation of inflammatory caspases and processing of proIL-beta. Mol Cell. 2002; 10:417–426. [PubMed: 12191486]

Martinon F, Mayor A, Tschopp J. The inflammasomes: guardians of the body. Annu Rev Immunol. 2009; 27:229–265. [PubMed: 19302040]

Mattson MP. Roles of the lipid peroxidation product 4-hydroxynonenal in obesity, the metabolic syndrome, and associated vascular and neurodegenerative disorders. Exp Geron. 2009; 44:625–633.

Maue AC, Yager EJ, Swain SL, Woodland DL, Blackman MA, Haynes L. T-cell immune senescence: lessons learned from mouse models of aging. Trends Immunol. 2009; 30:301–305. [PubMed: 19541537]

Maxfield FR, Tabas I. Role of cholesterol and lipid organization in disease. Nature. 2005; 438:612–621. [PubMed: 16319881]

Min H, Montecino-Rodriguez E, Dorshkind K. Reduction in the developmental potential of intrathymic T cell progenitors with age. J Immunol. 2004; 173:245–250. [PubMed: 15210781]

Morrissey P, Charrier K, Bressler L, Alpert A. The influence of IL-1 treatment on the reconstitution of the hemopoietic and immune systems after sublethal radiation. J Immunol. 1988a; 140:4204–4210. [PubMed: 3286769]

Morrissey PJ, Charrier K, Alpert A, Bressler L. In vivo administration of IL-1 induces thymic hypoplasia and increased levels of serum corticosterone. J Immunol. 1988b; 141:1456–1463. [PubMed: 3261749]

Nikolich-Zugich J, Slifka MK, Messaoudi I. The many important facets of T-cell repertoire diversity. Nat Rev Immunol. 2004; 4:123–132. [PubMed: 15040585]

Pang IK, Iwasaki A. Inflammasomes as mediators of immunity against influenza infection. Trends Immunol. 2011; 32:34–41. [PubMed: 21147034]

Pannetier C, Cochet M, Darche S, Casrouge A, Zoller M, Kourilsky P. The sizes of the CDR3 hypervariable regions of the murine T-cell receptor beta chains vary as a function of the recombined germ-line segments. Proc Natl Acad Sci USA. 1993; 90:4319–4323. [PubMed: 8483950]

Penack O, Holler E, van den Brink MR. Graft-versus-host disease: regulation by microbe-associated molecules and innate immune receptors. Blood. 2010; 115:1865–1872. [PubMed: 20042727]

Ramasamy R, Vannucci SJ, Yan SS, Herold K, Yan SF, Schmidt AM. Advanced glycation end products and RAGE: a common thread in aging, diabetes, neurodegeneration, and inflammation. Glycobiology. 2005; 15:16–28.

Sauce D, Larsen M, Fastenackels S, Duperrier A, Keller M, Grubeck-Loebenstein B, Ferrand C, Debré P, Sidi D, et al. Evidence of premature immune aging in patients thymectomized during early childhood. J Clin Invest. 2009; 119:3070–3078. [PubMed: 19770514]

Sempowski GD, Gooding ME, Liao HX, Le PT, Haynes BF. T cell receptor excision circle assessment of thymopoiesis in aging mice. Mol Immunol. 2002; 38:841–848. [PubMed: 11922942]

Shanley DP, Aw D, Manley NR, Palmer DB. An evolutionary perspective on the mechanisms of immunosenescence. Trends Immunol. 2009; 30:374–381. [PubMed: 19541538]

Sutterwala FS, Ogura Y, Szczepanik M, Lara-Tejero M, Lichtenberger GS, Grant EP, Bertin J, Coyle AJ, Galán JE, Askenase PW, et al. Critical role for NALP3/CIAS1/Cryopyrin in innate and adaptive immunity through its regulation of caspase-1. Immunity. 2006; 24:317–327. [PubMed: 16546100]

Tucker MZ, Turcotte LP. Aging is associated with elevated muscle triglyceride content and increased insulin-stimulated fatty acid uptake. *Am. J. Physiol*. Endocrinol Metab. 2003; 285:827–835.

Vandanmagsar B, Youm YH, Ravussin A, Galgani JE, Stadler K, Mynatt RL, Ravussin E, Stephens JM, Dixit VD. The NLRP3 inflammasome instigates obesity-induced inflammation and insulin resistance. Nat Med. 2011; 17:179–188. [PubMed: 21217695]

Williams KM, Hakim FT, Gress RE. T cell immune reconstitution following lymphodepletion. Semin Immunol. 2007; 19:318–330. [PubMed: 18023361]

Wu D, Ren Z, Pae M, Guo W, Cui X, Merrill AH, Meydani SN. Aging up-regulates expression of inflammatory mediators in mouse adipose tissue. J Immunol. 2007; 179:4829–4839. [PubMed: 17878382]

Yang H, Youm YH, Dixit VD. Inhibition of thymic adipogenesisby caloric restriction is coupled with reduction in age-related thymic involution. J Immunol. 2009; 183:3040–3052. [PubMed: 19648267]

Zhou R, Tardivel A, Thorens B, Choi I, Tschopp J. Thioredoxin-interacting protein links oxidative stress to inflammasome activation. Nat Immunol. 2010; 11:136–140. [PubMed: 20023662]

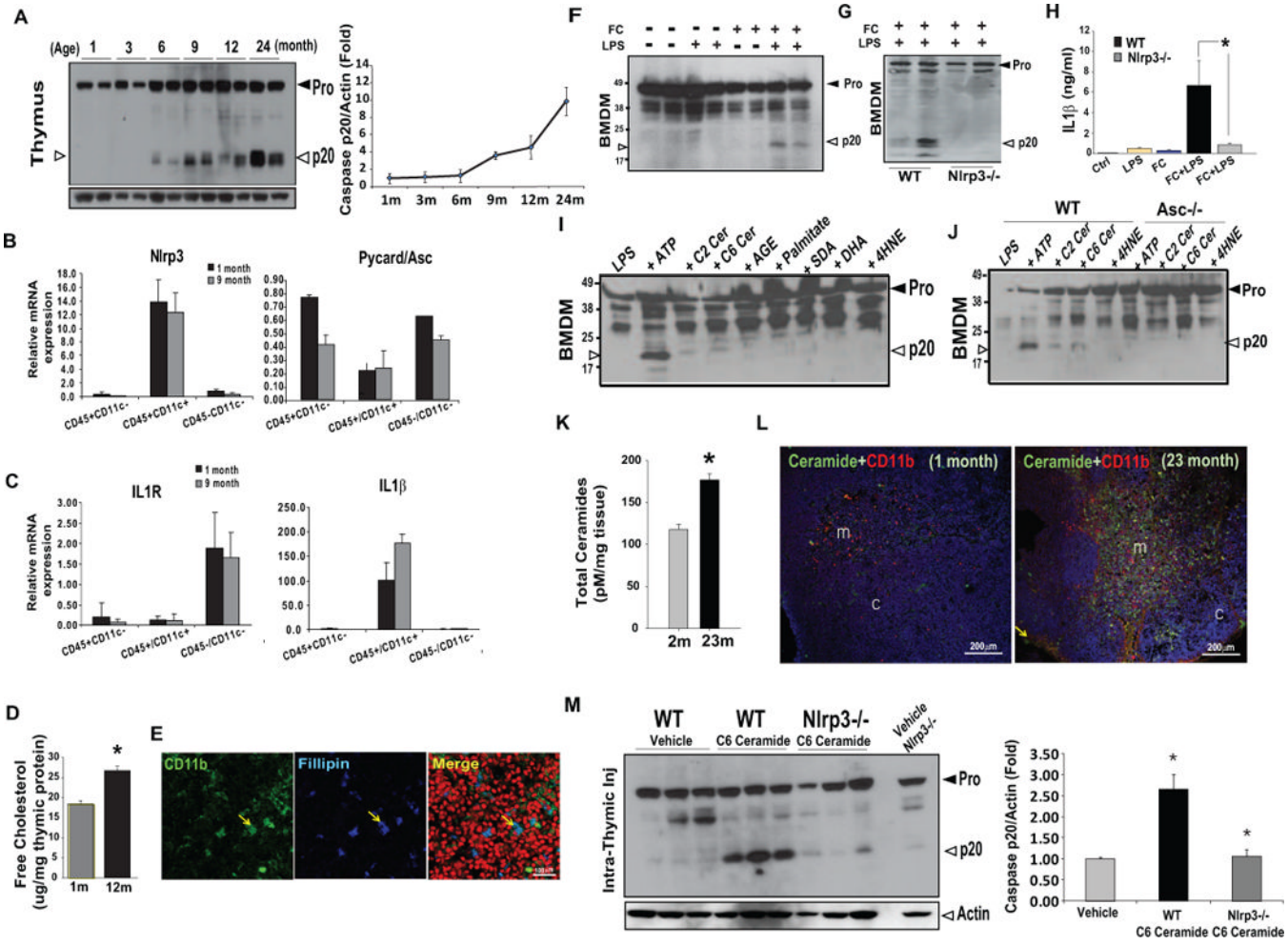


**Figure 1. Thymic aging is associated with the inflammasome activation**

(**A**) Western blot analysis of caspase-1 in thymus of C57/B6 mice from 1 month to 24 months of age. The experiment was repeated thrice from 3 different cohorts of mice and the data are expressed as fold change of active caspase-1 (p20) normalized to actin from a total of 6 mice per age point. (**B-C**) The thymocytes ($CD45^{+}CD11c^{-}$), thymic myeloid cells ($CD45^{+}CD11c^{+}$) and thymic stromal cells ($CD45^{-}CD11c^{-}$) from 1 and 9 month old mice (n = 6 each, repeated twice) were sorted using FACS. The total RNA was used for real-time PCR analysis of Nlrp3, Asc, IL-1R and IL-1β. The mRNA expression was normalized to *Gapdh* and shown as relative expression (ΔΔCt). Data are presented as means ± SD mean, $*P < 0.01$, (**D**) The free cholesterol levels in the thymi derived from 1month and 12 month old (n = 6/group) C57/B6 mice were measured using gas liquid chromatography. (**E**) The thymic cryosections from 24month old C57/B6 mice (n = 3) were imunostained with CD11b and filipin that binds to free cholesterol. The nuclei were counterstained with propidium iodide (red). The confocal immofluorescence analysis shows co-localization of macrophages with free cholesterol in medullary area of thymus. (**F**) The LPS primed BMDMs were loaded with methyl β-cyclodextrin-cholesterol (cholesterol concentration: 80mg/ml), which increases free cholesterol levels in BMDM to 60μg/mg protein (Supplementary Figure 1E). The cells were exposed to LPS for 6h and FC for 1h. The immunoblot analysis shows activated p20 form of caspase-1 in FC loaded LPS primed cells. (**G**) The western blot analysis of p20 subunit of caspase-1 in BMDMs from WT and *Nlrp3*$^{-/-}$ mice exposed to LPS and loaded with free cholesterol as described above. The 2 lanes represent 2 different

BMDM culture experiments from pooled cells of a total of 6 WT and 6 Nlrp3 KO mice (**H**) The IL-1β levels were determined by ELISA from supernatants of BMDMs derived from WT and *Nlrp3*$^{-/-}$ mice activated by LPS and FC (**I**) The immunoblotting for caspase-1 p20 in the LPS primed BMDMs treated with ATP (5mM), C2 ceramides (0.1mM), C6 ceramide (0.1mM), AGE (100μg/ml), BSA-conjugated palmitate (0.1mM), SDA (0.1mM), DHA (0.1mM) and 4HNE (50μg/ml). (**J**) The western blot analysis of p20 subunit of caspase-1 in BMDMs from WT and *Asc*$^{-/-}$ mice primed with LPS and treated with ATP, ceramides and 4HNE. The results are representative of 3 different experiments. (**K**) The total ceramides levels in thymi from 1month and 23month old thymi (n =6/group) were measured using LC/MS/MS. (**L**) The confocal immunofluorescence analysis of thymus labelled with anti-ceramide antibody (green, Alex Fluor488), anti-CD11b (red, Alexa Fluor 594) antibodies in 1 month and 23m old WT mice. Majority of staining (co-localization of ceramides and CD11b is indicated by yellow), was localized in thymic medulla (*m*) with little immune-reactivity in thymic cortex (*c*). DAPI (blue) was used to counterstain the nuclei. Representative image from a total of 4 sections from 3 mice each were used for confocal immunofluorescence analysis is shown. (**M**) The C6 ceramide (10mg/Kg b.w.) was injected intra-thymically in WT and *Nlrp3*$^{-/-}$ mice and thymi were collected after 1 hour for caspase-1 immunoblot analysis. The control mice were intrathymically injected with vehicle (alcohol). The quantification of p20 caspase-1 western blot band intensities were analyzed using ImageJ and arbitrary units were normalized to actin and expressed as fold change. All data are presented as means ± SEM, $*P < 0.05$.

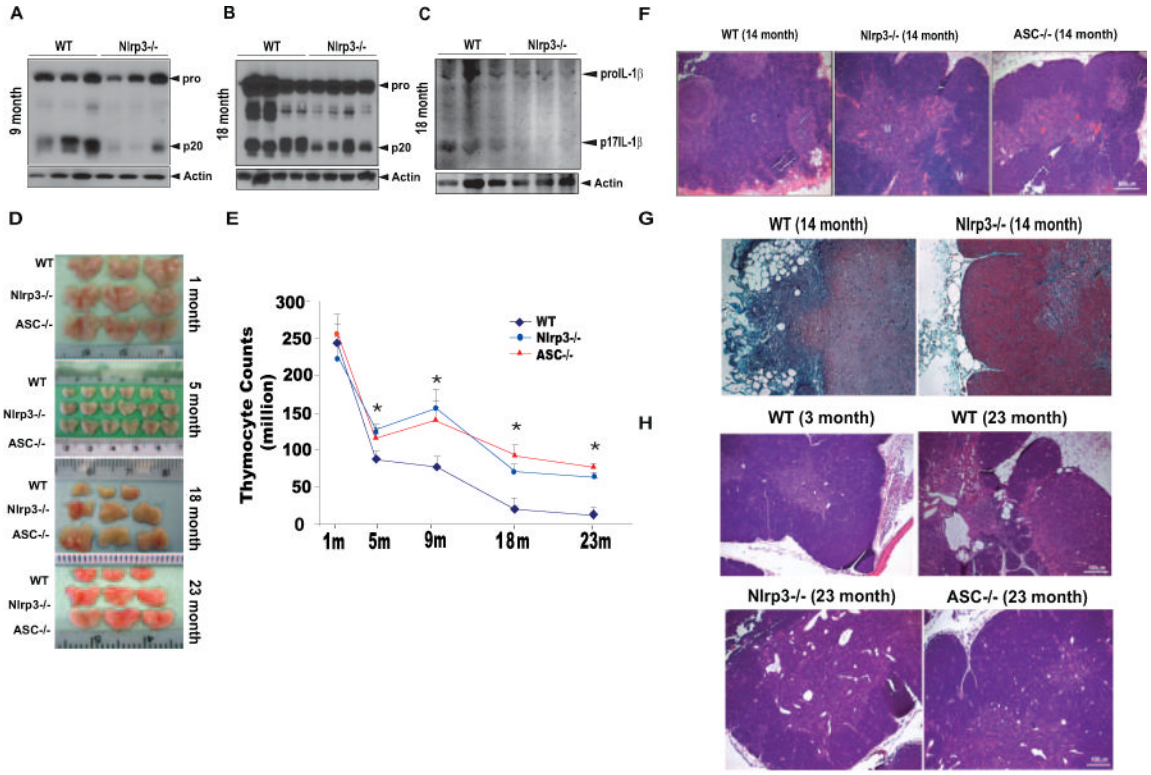


**Figure 2. The ablation of Nlrp3 inflammasome protects against age-related thymic involution**

The western blot analysis of caspase-1 activation in thymus of WT and *Nlrp3*$^{-/-}$ mice at (**A**) 9 months and (**B**) 18 months of age. (**C**) Immmunblot analysis of IL-1β activation in the thymi 18 month old WT and *Nlrp3*$^{-/-}$ mice. (**D**) Representative images showing the thymic size of WT, *Nlrp3*$^{-/-}$ and Asc$^{-/-}$ mice at 1, 5, 18 and 23 months of age (**E**) Total thymocyte counts in WT and *Nlrp3*$^{-/-}$ and Asc$^{-/-}$ mice at indicated ages (n = 6–12/age group). The thymocyte counts from 1 and 5 month old mice are from one cohort of mice (n =6/age group/strain). The data at each age point is analyzed from 2–3 cohorts (9 month old from 3 cohorts, 18 and 23month old from 2 cohorts) of mice sacrificed at least 6 months apart. (**F**) Representative H & E stained sections from 14m old *Nlrp3*$^{-/-}$ and Asc$^{-/-}$ mice (n =3–5). Loss of cortical regions (c) medullary areas (m) in WT mice is prevented in *Nlrp3*$^{-/-}$ and Asc$^{-/-}$. (**G**) The formalin fixed paraffin embedded (FFPE) thymi of 14 month old WT and *Nlrp3*$^{-/-}$ mice (n = 3/group) stained with Massons Trichome (light blue color indicates binding to collagen). The WT mice display greater subcapsular fibrosis and increase in ectopic adipocytes compared to age-matched *Nlrp3*$^{-/-}$ mice. (H) Representative H & E stained FFPE thymic sections of 23 month old WT and *Nlrp3*$^{-/-}$ and Asc$^{-/-}$ mice (n = 4/group). Compared to young (3 month) WT controls, age-related thymic involution is evident in 23 month old WT mice by loss of cortico-medullary junctions, complete loss of cortical regions and increase in thymic cysts and adipocytes.

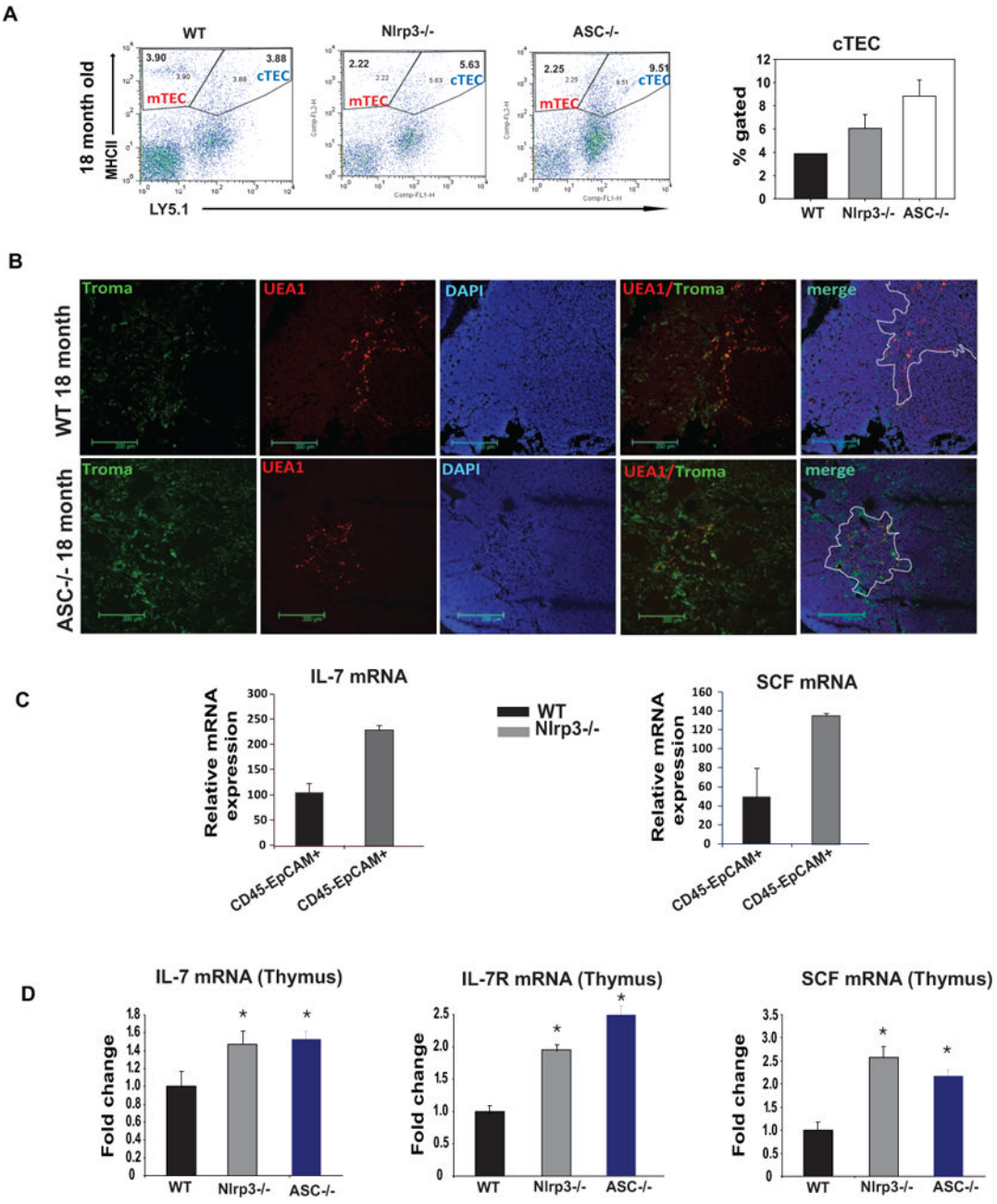


**Figure 3. Elimination of Nlrp3 inflammasome improves thymic stromal microenvironment in aging**

(**A**)The thymic cells from 18m old WT, *Nlrp3*$^{-/-}$ and Asc$^{-/-}$ mice were labelled with CD45, MHC-II and Ly5.1 to identify mTEC (CD45$^{-}$ MHCII$^{+}$Ly5.1$^{-}$) and cTEC (CD45$^{-}$MHCII$^{+}$Ly5.1$^{+}$) subsets. The expression of MHCII and Ly5.1 is analyzed on CD45 negative population. The percent gated cTEC cells are significantly (P<0.05) increased *Nlrp3*$^{-/-}$ and Asc$^{-/-}$ mice (n = 4–6/group). (**B**) Thymic sections from 18 month old WT and *Asc*$^{-/-}$ animals were used to stain for keratin 8$^{+}$ cortical TEC with anti-TROMA1 antibody and medullary TECs were identified by biotin conjugated plant lectin *Ulex europaeus agglutinin* 1 (UEA-1). Nuclei were counterstained with DAPI. In old WT mice, mTEC staining was localized on the periphery of medullary regions while in *Nlrp3*$^{-/-}$ mice,

medulla had diffuse UEA1 immuopositivity. (**C**) The $CD45^{-}EpCAM^{+}$ TECs from 12m old WT and *Nlrp3*$^{-/-}$ mice (n = 5/group) were isolated using FACS sorting and analyzed for IL-7, and SCF by real-time PCR analysis. (**D**) The IL-7, IL-7R and SCF mRNA in thymi of 9–10 month old WT, *Nlrp3*$^{-/-}$ and Asc$^{-/-}$ mice (n = 4–6/group) was analyzed using real-time PCR analysis. The mRNA expression was normalized to GAPDH expression and is shown as fold change $\Delta\Delta C_t$.

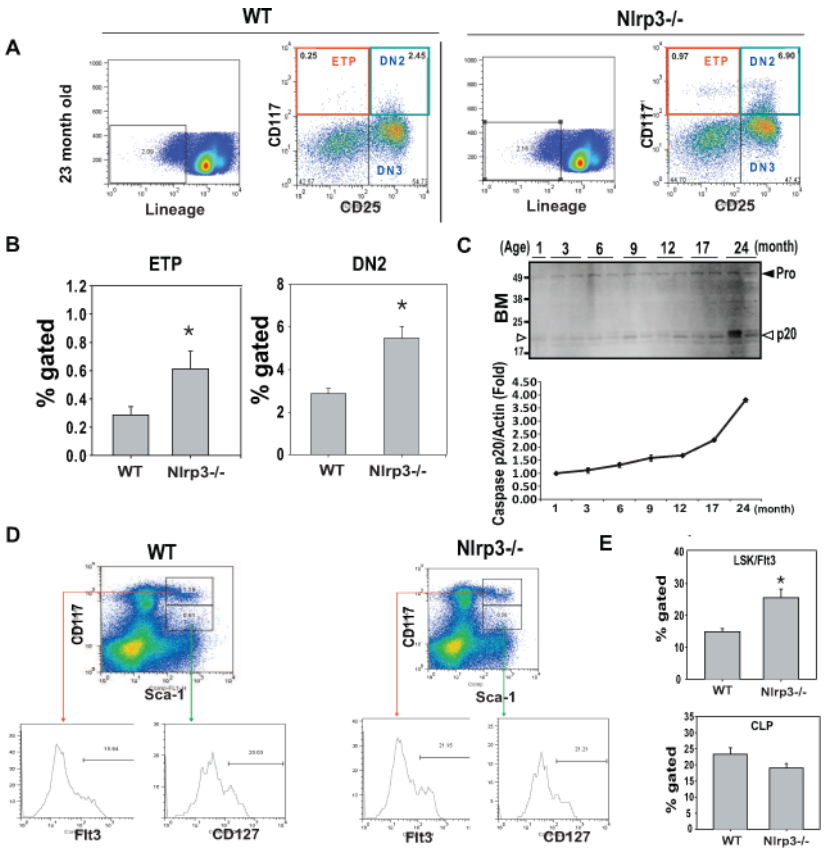


**Figure 4. Activation of Nlrp3 inflammasome reduces T cell progenitors in aging**

(**A**) The thymocytes from 23 month old WT and *Nlrp3*$^{-/-}$mice (n = 4–6/group) were stained to identify earliest thymocyte progenitors (Lin$^{lo}$CD117$^{+}$CD25$^{-}$) and DN2 (Lin$^{lo}$CD117$^{+}$CD25$^{+}$) and DN3 (Lin$^{lo}$CD117$^{-}$CD25$^{+}$) cells. (**B**) There is a significant increase (P<0.05) in percent gated ETPs and DN2 cells in the thymi of aged *Nlrp3*$^{-/-}$ mice. (**C**) Western blot analysis of caspase-1 activation in bone marrow during aging. The activated p20 active form is shown by arrow heads. (**D**) Representative FACS dot plots show the analysis of MPP (Lin$^{lo}$Sca1$^{+}$kit$^{+}$Flt$^{+}$) and CLP (Lin$^{lo}$Sca1$^{+}$kit$^{lo}$CD127$^{+}$) cells in BM of 22month old WT and *Nlrp3*$^{-/-}$mice. The Flt3 and CD127 expression on these subpopulation are depicted as histograms. (**E**) There is a significant increase (P<0.05) in percent gated MPP cells but no change in CLPs in aged *Nlrp3*$^{-/-}$mice. (n = 6/group)

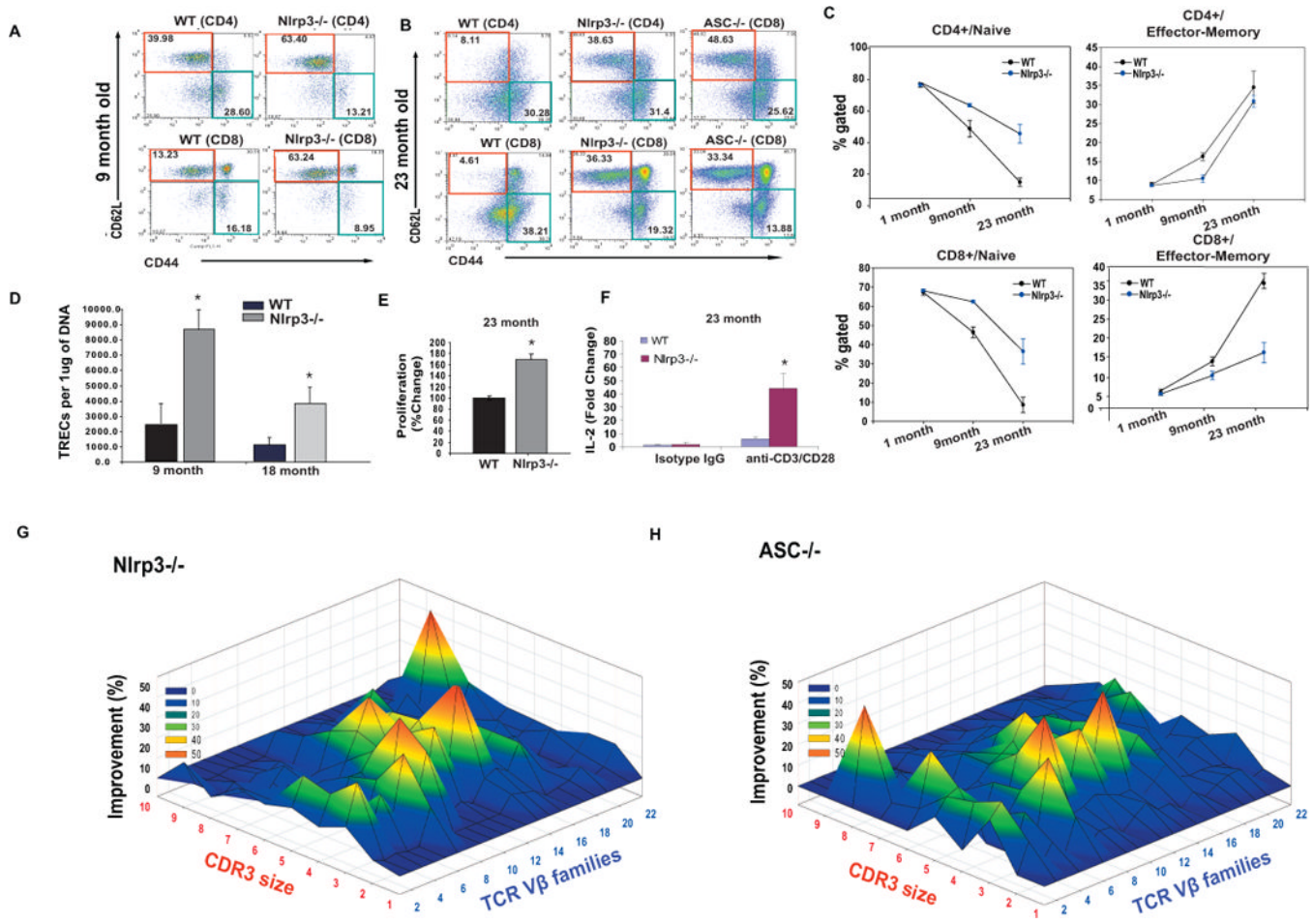


**Figure 5. Ablation of Nlrp3 inflammasome protects against immune-senescence and loss of TCR diversity in aging**

(**A**) The splenocytes were stained with CD4, CD8, CD62L and CD44 to identify naïve (CD4/CD8$^-$CD62L$^+$CD44$^-$) and E/M (CD4/CD8$^-$ CD62L$^+$CD44$^-$) T cells. The representative FACS dot plots from 9 month WT and *Nlrp3*$^{-/-}$mice, (**B**) 23 month old WT, and age-matched *Nlrp3*$^{-/-}$ and *Asc*$^{-/-}$ mice. (**C**) Kinetics of CD4 and CD8 naïve and E/M cells in WT and *Nlrp3*$^{-/-}$mice during aging. (**D**) The quantitative -PCR analysis of signal-joint TREC levels in splenic CD4$^+$ T cells in 9m and 18m old WT and *Nlrp3*$^{-/-}$mice. (**E**) The splenic T cells derived from 23 month old WT and *Nlrp3*$^{-/-}$mice were stimulated by plate bound anti-CD3 and CD28 antibodies to mimic TCR ligation and cell growth/ proliferation was measured using MTT assay. (**F**) The real time PCR analysis of IL-2 mRNA from unstimulated and activated (via plate bound anti-CD3 and CD28 antibodies) from 23 month old WT *and Nlrp3*$^{-/-}$ mice. (**G**) The TCR spectratyping analysis of CD4 T cells from 23 month old WT and *Nlrp3*$^{-/-}$ mice (n = 3/group). The improvement in TCR diversity are depicted as landscape surfaces, in which smooth (blue) landscapes represent an unchanged TCR repertoire (diversity). The Mountain (in green, yellow and orange) depicts area under the curve (AUC) of Gaussian amplified peaks of CDR3 lengths. Each line crossing on the *y* axis of the landscape denotes change from WT specific CDR3 length or size (*x*-axis) of a particular Vβ family (*z*-axis). (n = 3/group)

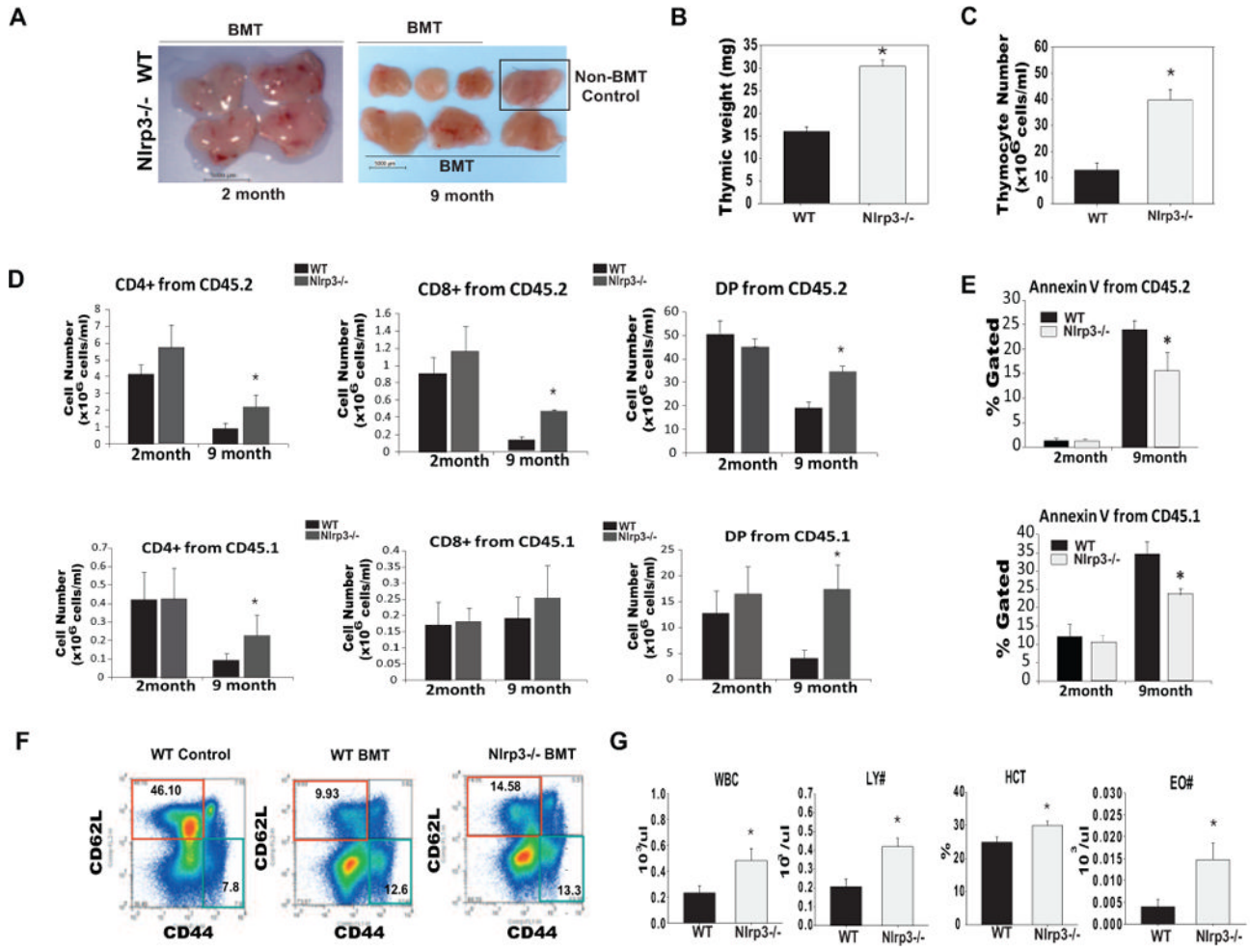


**Figure 6. Elimination of Nlrp3 inflammasome promotes T cell reconstitution postirradiation and HSCT**

(**A**) Thymic size of 2 month and 9 month old WT and *Nlrp3*$^{-/-}$ 2 weeks after irradiation and BMT. (**B**) Thymic weight (**C**) thymocyte numbers in 9 month old WT and *Nlrp3*$^{-/-}$ mice 2 weeks after 750cGy irradiation and BMT. (**D**) The thymocytes from 2 and 8–9 months old WT and *Nlrp3*$^{-/-}$ were stained with CD45.1 (for donor cells), CD45.2 (for host cells), CD4 and CD8. The total thymocyte subset numbers gated on donor and host cells from young and middle-aged WT and *Nlrp3*$^{-/-}$ mice are shown (n = 5–7). The BMT experiments were repeated twice in 2 different cohorts of 8–9 month old WT and *Nlrp3*$^{-/-}$ mice. (**E**) To examine cell death in WT and *Nlrp3*$^{-/-}$ mice undergoing irradiation and BMT, the thymocytes from 2 month and 8–9 month old WT and *Nlrp3*$^{-/-}$ were stained for Annexin-V, CD45.1 (donor), CD45.2 (host). The percent Annexin-V$^{+}$ thymocytes from young and middle-aged WT and *Nlrp3*$^{-/-}$ mice are shown (n = 5–7). (**F**) The splenocytes from 9 month old WT and WT and *Nlrp3*$^{-/-}$ mice were stained with CD3, CD62L and CD44 to identify naïve (CD3$^{-}$ CD62L$^{+}$CD44$^{-}$) and E/M (CD3 $^{-}$CD62L$^{+}$CD44$^{-}$) T cells. (**G**) The complete blood count (CBC) analysis in peripheral blood of 9 month old WT and *Nlrp3*$^{-/-}$mice 2 weeks after radiation and BMT. All data are presented as means ± SEM, **P* < 0.05 (n = 6–8/ group).